

**Stability line of liquid molecular nitrogen based on the SCAN meta-GGA density functional**G. Zhao,<sup>1,\*</sup> H. Wang,<sup>2</sup> M. C. Ding,<sup>1</sup> X. G. Zhao,<sup>1</sup> H. Y. Wang,<sup>1</sup> and J. L. Yan<sup>1</sup><sup>1</sup>*School of Physics and Optoelectronic Engineering, Ludong University, Yantai 264025, People's Republic of China*<sup>2</sup>*Department of Electronic Engineering, Yantai Automobile Engineering Professional College, Yantai 265500, People's Republic of China*

(Received 6 August 2018; revised manuscript received 2 October 2018; published 20 November 2018)

It was recently reported in experiments that at temperatures below 2500 K liquid nitrogen (N) remains molecular up to 120 GPa [Phys. Rev. Lett. **119**, 235701 (2017)], which contradicts a liquid-liquid transition at 88 GPa and 2000 K predicted by PBE-GGA density functional. To clarify this, we perform extensive first principles molecular dynamics using SCAN meta-GGA density functional, which captures the intermediate-range part of the van der Waals interaction better than PBE-GGA. It is found that SCAN gives more accurate bond energy and length of an isolated N<sub>2</sub> molecule than PBE. SCAN, as well as PBE, is capable of reproducing the first-order molecular-to-polymeric phase transition, but in contrast to PBE, it predicts a wider stability range for fluid N<sub>2</sub>. The boundary of this range is 15 GPa higher than the one predicted with PBE, which is in closer agreement with experiments. In addition, SCAN predicts a higher amount of threefold coordinated atoms in the polymeric phase than PBE, which is expected from experiments in amorphous N. These improvements indicate that SCAN is more accurate than PBE in predicting the phase transition from molecular to polymeric fluid N.

DOI: [10.1103/PhysRevB.98.184205](https://doi.org/10.1103/PhysRevB.98.184205)**I. INTRODUCTION**

The evolution of simple molecular systems upon compression is of fundamental scientific and technological importance contributing to the field condensed matter physics and material sciences. In this regard, nitrogen (N) is consistently considered as a model system, as it forms the most strongly triple-bonded simple molecule at low pressures. The destabilization of N  $\equiv$  N triple bonds upon compression leads to the transition to nonmolecular single-bonded polymeric phase [1], which has been intensively investigated as a high energy-density material [2–13]. The cubic gauche (cg) N was found to be energetically the most stable one after the breakdown of the molecular phases [4]. However, about the transition pressure, there are considerable disagreements between the experimental observations and theoretical predictions. The calculations predicted that the transformation from molecular to nonmolecular solid occurs at pressures of 50–75 GPa [1–4], but experimentally this was not observed until 190 GPa at 80 K and near 150 GPa at 300 K, where the transition to an amorphous polymeric phase occurs [14]. Eventually, Eremets *et al.* synthesized the cg-N directly from the molecular N above 2000 K at 115 GPa [15], much higher than the predicted transition pressure.

More recently, similar disagreements have also been reported in liquid N. First-principles simulations provided direct evidence for a first-order transition from molecular to polymeric fluid N [16], which is related to the maximum melting temperature of the solid molecular N between 80 and 90 GPa [17]. However, in experiments, neither the Raman studies [18,19] nor the recent synchrotron x-ray diffraction measurements in 2017 [20] found evidence of polymeric fluid

N up to 120 GPa, although a maximum on the melting curve was found at much lower pressure (70 GPa for Refs. [18,19] and 50 GPa for Ref. [21]). It should be noted that the synchrotron x-ray diffraction measurements have found no evidence of a maximum on the melting curve [20]. These experimental observations contradict the theoretical prediction and make the predicted first-order liquid-liquid transition at 88 GPa, 2000 K [16] doubtful.

The disagreement between theory and experiment is usually considered to be linked to the high energy barrier of transitions, which results in the metastability of phases [14]. For a given temperature, DFT simulations can predict the pressure at which the transition takes place, that is, the pressure at which the two phases coexist in equilibrium. However, due to the high-energy barrier of the transition, N can remain molecular beyond the transition pressure, in a metastable phase whose stability region is bounded by the spinodal line, which is regarded as the stability boundary of metastable molecular N. Whether this discrepancy in the transition pressure between theory and experiments comes from this distinction, or from inherent errors associated with the choice of the exchange-correlation functional in DFT, is something that must be investigated. Clarification of this question is crucial for assessing the reliability and accuracy of theoretical calculations for the related transition in molecular N and for understanding the kinetics of high-pressure transformations.

Over the past decade, the PBE-GGA [6–12,16,17,22] has replaced LDA [2–5] as a widely used density functional for the study of molecular and polymeric N. In molecular N, the strong N  $\equiv$  N triple bonds coexist with weak van der Waals interactions between molecules. It was recently shown that the van der Waals interactions can widen the thermodynamical stability region of the molecular phase [23]. However, PBE-GGA largely loses the intermediate-range van der Waals interaction, although it has been verified more accurate than

\*gzhao19800209@126.com

LDA for a wide range of systems, with nitrogen clusters being one of them. Recently, Sun *et al.* [24,25] developed a strongly constrained and appropriately normed (SCAN) meta-GGA functional, which satisfies all 17 known exact constraints on semilocal exchange-correlation functionals and is able to capture the intermediate-range part of the van der Waals interaction better. Although it has been shown to be superior to PBE-GGA for predicting the accurate geometries and energies of diversely bonded molecules and materials (including covalent, metallic, ionic, hydrogen, and van der Waals bonds) [24–26] at nearly the same computational cost, the predictive accuracy of SCAN meta-GGA for phase transitions in liquids, which require an accurate simultaneous description of different bonding types, needs to be further explored.

In this work, the SCAN meta-GGA is used to revisit the first-order phase transition in liquid N by performing extensive first-principle molecular dynamics simulations. We find that SCAN provides a better description of the isolated  $N_2$  molecule than PBE, as the bond length and binding energy are in closer agreement with experimental data. SCAN, as well as PBE, is also able to reproduce the first-order molecular-to-polymeric phase transition, but in contrast to PBE, it predicts a wider stability range for fluid  $N_2$ . The boundary of this range is 15 GPa higher than the one predicted with PBE, which is in closer agreement with experiments. In addition, SCAN predicts a higher amount of threefold coordinated atoms in the polymeric phase than PBE, which is expected from experiments in amorphous N. These improvements indicate that SCAN is more accurate than PBE in predicting the phase transition from molecular to polymeric fluid N.

## II. SIMULATION DETAILS

For our first principles molecular dynamics simulations, we use the Vienna *ab initio* simulation package (VASP) [27,28] together with projector augmented wave (PAW) potential [29]. The SCAN meta-GGA [24,25] and PBE-GGA [30] are both used for comparison. It is found that the wall time using SCAN meta-GGA is about three times that of using PBE-GGA under the same conditions. The electronic wave functions are expanded in the plane wave basis set with an energy cutoff of 700 eV, which is larger than that used in Ref. [16] (500 eV) and is enough to give an accurate value of calculated pressure without Pulay correction (see below). The simulations are performed in the canonical (NVT) ensemble with a 64-atom supercell and a Nosé thermostat for temperature control [31]. We explored size effects by performing simulations in a 48 and 128 atoms supercells at 2200 K. The Gamma point is used to sample the Brillouin zone in all cases. At each state point, the simulation runs for at least 30 ps with a 1.0 fs ionic time step. Near the phase transition region, the simulation of 64-atom supercell runs for 120 ps at most.

## III. RESULTS AND DISCUSSION

We studied the bond energy and bond length of the  $N_2$  molecule using both PBE and SCAN functionals. The results are shown in Fig. 1, together with the experimental result. Our calculations show that PBE predicts a bond length of 1.114 Å and bond energy of 1001.35 kJ/mol, while SCAN predicts

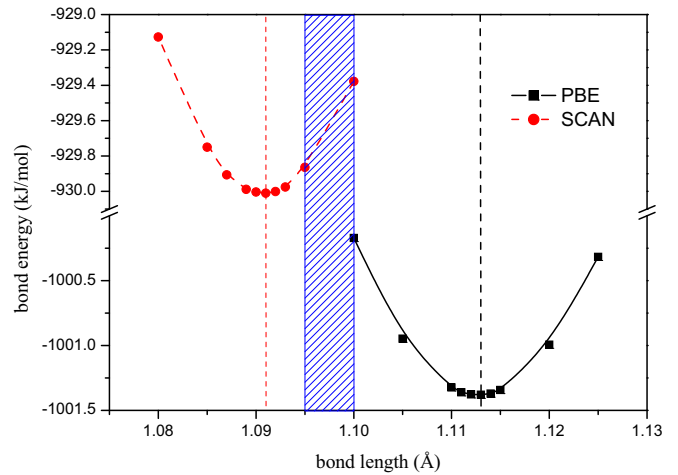


FIG. 1. The  $N \equiv N$  bond energy as a function of bond length in an isolated  $N_2$  molecule based on PBE and SCAN, respectively. PBE gives 1001.35 kJ/mol and 1.114 Å, while SCAN gives 930 kJ/mol and 1.091 Å, which is closer to the experimental data [32], 941 ~ 954 kJ/mol and 1.095 ~ 1.10 Å, and indicates that SCAN is better than PBE in describing the isolated  $N_2$  molecule. The blue shadow indicates the range of the bond length obtained in experiments [32].

1.091 Å and 930 kJ/mol. Comparing with the experimental data [32], which predicts a bond length of 1.095 ~ 1.10 Å and binding energy of 941 ~ 954 kJ/mol, we conclude that SCAN predicts more accurate values than PBE. It should be mentioned that, despite the closer agreement with experiments [32], SCAN functional underestimates the bond length and bond energy, outside the error bars of the experiment.

Our calculated compression isotherms at 2000 K based on SCAN and PBE are both presented in Fig. 2. The simulation atomic volume ranges from about 5.5 to 8.0 Å<sup>3</sup>/atom,

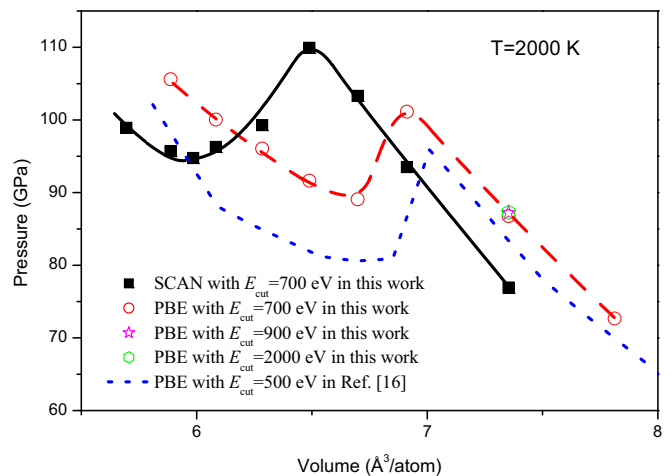


FIG. 2. The calculated compression isotherms at 2000 K based on SCAN meta-GGA (black solid square) and PBE-GGA (red solid circle), together with the results of 500 eV energy cutoff based on PBE-GGA (blue dotted line) in Ref. [16]. For PBE-GGA, the energy cutoff of 500 eV gives lower pressure than that of 700 eV. Compared with PBE-GGA, SCAN meta-GGA gives the lower pressure and a maximum at higher pressure.

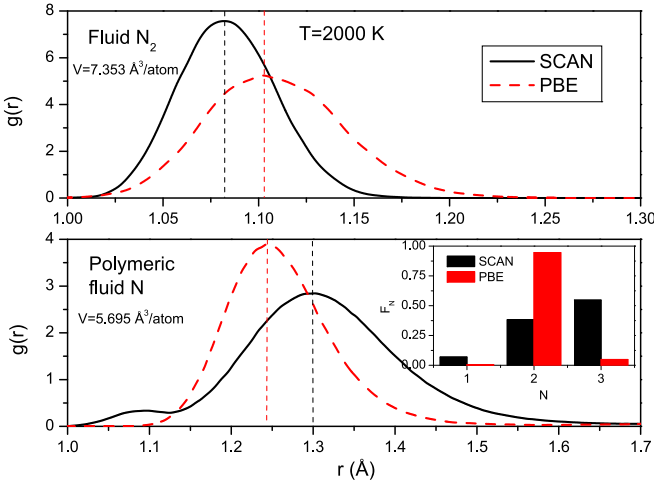


FIG. 3. Upper: Pair correlation function  $g(r)$  in fluid  $N_2$  at  $V = 7.353 \text{ \AA}^3/\text{atom}$  and  $T = 2000 \text{ K}$ , indicating more stable  $N \equiv N$  triple bonds described by SCAN meta-GGA. Lower: Pair correlation function  $g(r)$  and the fraction of  $n$ -coordinated atoms  $F_n$  (inset) in polymeric fluid N at  $V = 5.695 \text{ \AA}^3/\text{atom}$  and  $T = 2000 \text{ K}$ . The atoms are mainly two-coordinated for PBE-GGA, while for SCAN meta-GGA, three-coordinated atoms are the majority and there remain some one-coordinated atoms.

which is largely smaller than that of liquid  $N_2$  at  $77 \text{ K}$ ,  $28.77 \text{ \AA}^3/\text{atom}$ . For comparison, the calculated results of 64 atoms and 500 eV energy cutoff based on PBE in Ref. [16] are also shown. It can be seen that the three isotherms all show van der Waals loops, indicating the nature of a first-order phase transition. However, for the two isotherms based on PBE, using an energy cutoff of 500 eV gives lower pressures than using 700 eV. The corresponding transition pressure, determined by Maxwell's equal areas construction, is 6 GPa higher when a 700 eV is used as energy cutoff. Simulations of warm dense nitrogen based on PBE [22], using an energy cutoff of 2000 eV, have also explored the molecular-to-polymeric phase transition of N. It was also observed that the transition pressure is about  $6 \sim 7 \text{ GPa}$  higher than the results in Ref. [16] with an energy cutoff of 500 eV. At  $T = 2000 \text{ K}$  and  $V = 7.353 \text{ \AA}^3/\text{atom}$ , our calculated pressures with different energy cutoff (also shown in Fig. 2) are 86.9 GPa (700 eV), 87.2 GPa (900 eV), and 87.3 GPa (2000 eV), respectively. Comparing these values with the pressure obtained in Ref. [16] using only 500 eV (84 GPa), we can conclude that this energy cutoff is not sufficient to obtain well converged pressures. Our choice of 700 eV is, then, chosen for the rest of our calculations.

Compared with PBE, SCAN gives lower pressures at the same volume and temperature for both low- and high-density phases in Fig. 2. The reasons for this can be obtained qualitatively by the analysis of the structure shown in Fig. 3. For low-density fluid  $N_2$ , the first peak of pair correlation function  $g(r)$  in SCAN is located at about  $1.08 \text{ \AA}$ , while at  $1.10 \text{ \AA}$  in PBE. This means that, due to the effect of pressure, the bond length in fluid  $N_2$  is slightly less than that in an isolated  $N_2$  molecule. However, the result that the bond length in SCAN is shorter than that in PBE is consistent with that in the calculation of an isolated  $N_2$  molecule. Moreover,

the former is higher in height and narrower in width. These features indicate a smaller value of  $b$  (the average excluded volume per mole of N atoms) in the van der Waals equation  $(P + a/V_m^2)(V_m - b) = RT$  and so a smaller pressure for SCAN. For high-density polymeric fluid N, the main peak of  $g(r)$  in SCAN is located at  $1.30 \text{ \AA}$ , larger than that in PBE  $1.24 \text{ \AA}$ , with a wider peak of less height. However, the fraction of  $n$ -coordinated atoms ( $F_n$ ), presented in the inset, shows that the atoms are mainly two-coordinated in the polymeric fluid N described by PBE, while in that described by SCAN, three-coordinated atoms are the majority and there remain some one-coordinated atoms. The calculated  $b$  based on SCAN is approximately equal to  $2.45 N_A \text{ \AA}^3$ , which is less than that based on PBE ( $\approx 2.61 N_A \text{ \AA}^3$ ) and also leads to less pressure. Based on  $g(r)$ , the average coordination number (CN) can be calculated by the equation,  $CN = \int_0^{r_{\text{cutoff}}} 4\pi r^2 \rho g(r) dr$ , where  $\rho$  is number density of the atoms and  $r_{\text{cutoff}}$  is the cutoff distance. Here,  $r_{\text{cutoff}}$  is chosen to be the position of the first minimum of  $g(r)$ . Our calculated CN is 2.06 for PBE and 2.47 for SCAN. The previous experimental result of CN is about 2.5 in solid amorphous nitrogen observed near 150 GPa and low temperature [33]. Because of the similarity between liquid and amorphous structures, we think that SCAN can describe the structure of polymeric fluid N more accurately. We notice that the previous first-principle molecular dynamics simulations with PBE and an energy cutoff of 500 eV also showed many three-coordinated atoms in polymeric fluid N and CN is larger than 2 [16]. Here, we checked this question and it is found that when the used energy cutoff is 500 eV, CN is 2.38, indeed larger than 2. Comparing with the result of CN with the energy cutoff of 700 eV (2.06), we think that the difference between them is caused by the incompleteness of the plane wave basis set with the energy cutoff of 500 eV and the result that CN is 2.38 can be misleading information.

Now we turn to the study of the stability region of fluid  $N_2$ . In the  $P$ - $T$  plane, the limit of stability, or spinodal line, is the locus of points  $P_s(T)$  or  $T_s(P)$ , where  $(\partial P/\partial V)_T = 0$ . Along an isotherm  $P(V)$  at a fixed temperature  $T_0$ ,  $P_s(T_0)$  can be identified as the extremum [34,35]. Based on the compression isotherms in Fig. 2, one can locate the maxima as the spinodal points of fluid  $N_2$  at 2000 K. It can be seen that the pressure of the spinodal point for SCAN is about 10 GPa higher than that for PBE, meaning that the stability region of fluid  $N_2$  based on SCAN is larger than that based on PBE. To obtain the spinodal line of fluid  $N_2$  in the  $P$ - $T$  plane, the isothermal compression of 64-atom supercell is simulated at eight temperatures ranging from 2000 to 7000 K, as shown in Fig. 4. It can be seen that the isotherms from 2000 to 4000 K all show a van der Waals loop, indicating the nature of a first-order phase transition, however, from 5000 to 7000 K they do not exhibit a drop in pressure. This means the existence of a critical point at  $4000 < T_c < 5000 \text{ K}$ , consistent with that obtained by Boates and Bonev in PBE-GGA first-principle molecular dynamics [16]. In addition, Boates and Bonev also reported that above 5000 K, the temperature-driven dissociation of  $N_2$  inhibits the formation of extended structures and leads to form liquid atomic N. Here, based on SCAN meta-GGA, it is found that at the inflection point of the isotherm,  $N_2$  molecules begin to be destroyed and

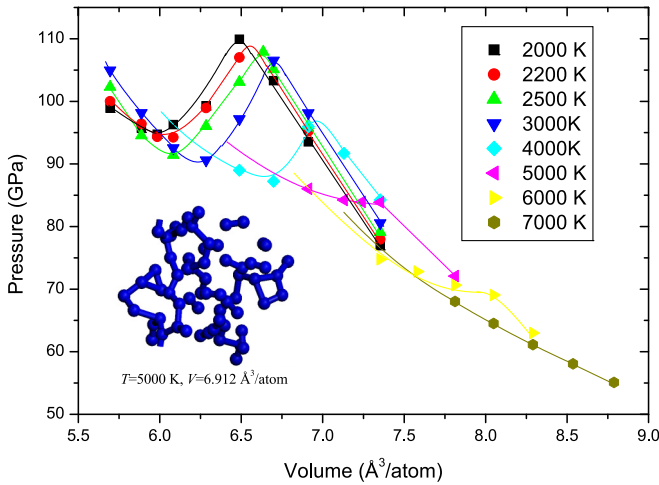


FIG. 4. The calculated compression isotherms at eight temperatures based on SCAN meta-GGA. From 2000 to 4000 K, a van der Waals loop is presented and the maximum is located as the spinodal point of fluid  $N_2$ . However, from 5000 to 7000 K the isotherms do not exhibit a drop in pressure, meaning the existence of a critical point at  $4000 < T_c < 5000$  K. Inset: Snapshot of the structure of fluid N at  $T = 5000$  K and  $V = 6.912 \text{ \AA}^3/\text{atom}$ . It is a mixture of molecular and polymeric N and no liquid atomic N is found.

two-coordinated atoms occur. No liquid atomic N is found at higher pressures along isotherms above 5000 K, while the liquid is the mixture of molecular and polymeric N, shown in the inset of Fig. 4. The spinodal points of fluid  $N_2$  determined by the maxima of the compression isotherms are shown in Fig. 5. For comparison, the stability region based on PBE in Ref. [16,36] and experiments in Refs. [14,15,20,37] are also shown in Fig. 5, together with the experimental [18–21] and theoretical [17] melting curve. It is important that, by contrast with PBE, the stability line of fluid  $N_2$  based on SCAN shifts about 15 GPa towards high pressure, closer to our proposed line based on experimental observations. Especially at about 2000 K, our result 110 GPa is very close to the experimental result 115 GPa [14,15]. At high temperature, there is a big difference between theory and experiment. However, the experimental results vary greatly in different experiments, for example, 7000 K, 90 GPa in Ref. [37] and 6000 K, 30 GPa in Ref. [38]. Thus, more accurate experimental measurements are needed at high temperatures. Correspondingly, the critical point and the phase transition line estimated by Maxwell's equal areas construction also shift more than 10 GPa towards high pressure.

Although the stability line of fluid  $N_2$  based on SCAN is more accurate than that based on PBE, there still exists a slight difference that cannot be ignored between our calculated results and experimental observation. This may originate from the following two aspects. First, as demonstrated in Ref. [39], the extrema of the finite size equilibrium isotherm is actually system-size dependent. Only for small enough systems, a smooth van der Waals-type isotherm can be found and the extrema can indeed be reached up to almost the spinodal point. Here, we compare the compression isotherms of 48-, 64-, and 128-atom supercell along 2200 K, shown in

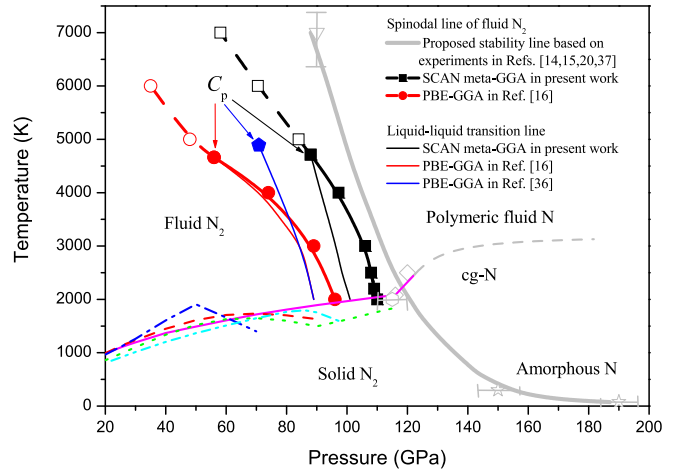


FIG. 5. The stability line of fluid  $N_2$  in phase diagram. The spinodal points (solid symbols) below critical point ( $C_p$ ) bounds the stability region of fluid  $N_2$  and the open symbols are the inflection points of the isotherms above  $C_p$ . Lines joining the symbols are guides to the eye. The melting curves obtained from Raman experiments (red dash line and green short dash line) [18,19], synchrotron x-ray diffraction (thin magenta line) [20], optical measurements (blue dash dot line) [21], and DFT based on PBE (cyan dash dot dot line) [17] are also shown. Comparing our SCAN-based results with previous PBE-based results [16,36], we observe that the stability line of fluid  $N_2$  shifts about 15 GPa towards high pressure, closer to the proposed stability line. The proposed stability line is based on experimental results from ultrahigh-pressure electrical resistance measurements (pentagon) [14], x-ray diffraction (hexagon) [15], synchrotron x-ray diffraction (diamond) [20], and shockwave experiments (triangle) [37].

Fig. 6. It can be found that with decreasing the number of atoms, the maximum tends to higher pressure. So, when a smaller system (48 atoms) is simulated, the spinodal line will be closer to experimental observations. Especially at about 2000 K, our calculated result 112 GPa is nearly the same as

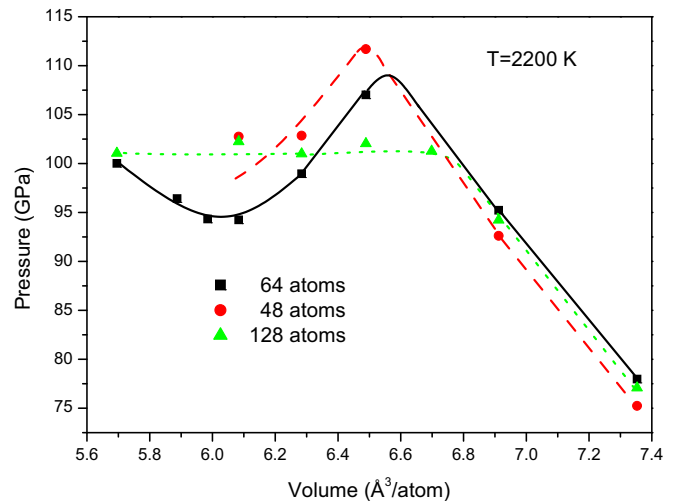


FIG. 6. Comparison of the compression isotherms for 48-, 64-, and 128-atom supercells at 2200 K. With decreasing the number of atoms, the maximum tends to higher pressure.

the experimental result 115 GPa [15] within the margin of error. However, it should be mentioned that, as convergence with respect to the number of particles cannot be clearly determined, the good agreement of our calculated pressure (112 GPa) for 48 particles with experiments (115 GPa) is thus somewhat fortuitous. Second, the SCAN meta-GGA density functional is not perfect, which can be seen from the result of the calculation for an isolated  $N_2$  molecule. In addition, although SCAN captures much of the intermediate-range part of the van der Waals interaction, it still cannot capture the long-range part. This can also have influence on the study of the stability of fluid  $N_2$ .

#### IV. CONCLUSIONS

In conclusion, the extensive SCAN meta-GGA first-principle molecular dynamics simulations are performed to revisit the first-order phase transition in liquid N. It is found that SCAN gives more accurate bond energy and length of an isolated  $N_2$  molecule than PBE. SCAN, as well as PBE, is capable of reproducing the first-order molecular-to-polymeric phase transition, but in contrast to PBE, it predicts a wider stability range for fluid  $N_2$ . The boundary of this range is 15 GPa higher than the one predicted with PBE, which is in closer agreement with experiments. In addition, SCAN predicts a higher amount of threefold coordinated atoms in the polymeric phase than PBE, which is expected from

experiments in amorphous N. These improvements indicate that SCAN is more accurate than PBE in predicting the phase transition from molecular to polymeric fluid N.

The liquid-liquid phase transition is usually considered to be related to the maximum of the melting curve. However, the recent synchrotron x-ray diffraction measurements did not find the maximum up to 116 GPa [20]. So its existence and the relation between it and the phase transition need to be further studied by SCAN. In addition, the better description of polymeric fluid N by SCAN indicates that it can also be the same in polymeric solid N. As potential high-energy-density materials, the present work would stimulate the study of their low-pressure stability and the prediction of new high-pressure polymeric structure by SCAN. Besides  $N_2$ , the phase transition in other liquid molecular systems, such as  $H_2O$ ,  $H_2$ ,  $P_4$ , etc., should be further studied based on SCAN in the future. Especially for  $H_2O$ , whether there exists a liquid-liquid critical point and where it is located are key for understanding its anomalous thermodynamic properties.

#### ACKNOWLEDGMENTS

This work is supported by National Natural Science Foundation of China (Grants No. 11504154 and No. 11874191) and Natural Science Foundation of Shandong Province of China (Grant No. ZR2016FM38). This work was completed on the Tianhe-2 supercomputer in LvLiang Cloud Computing Center located at Lvliang City, Shanxi Province, China.

- 
- [1] A. K. McMahan and R. LeSar, *Phys. Rev. Lett.* **54**, 1929 (1985).  
 [2] R. M. Martin and R. J. Needs, *Phys. Rev. B* **34**, 5082 (1986).  
 [3] S. P. Lewis and M. L. Cohen, *Phys. Rev. B* **46**, 11117 (1992).  
 [4] C. Mailhot, L. H. Yang, and A. K. McMahan, *Phys. Rev. B* **46**, 14419 (1992).  
 [5] M. M. G. Alemany and J. L. Martins, *Phys. Rev. B* **68**, 024110 (2003).  
 [6] W. D. Mattson, D. Sanchez-Portal, S. Chiesa, and R. M. Martin, *Phys. Rev. Lett.* **93**, 125501 (2004).  
 [7] F. Zahariev, A. Hu, J. Hooper, F. Zhang, and T. Woo, *Phys. Rev. B* **72**, 214108 (2005).  
 [8] A. R. Oganov and C. W. Glass, *J. Chem. Phys.* **124**, 244704 (2006).  
 [9] Y. Yao, J. S. Tse, and K. Tanaka, *Phys. Rev. B* **77**, 052103 (2008).  
 [10] C. J. Pickard and R. J. Needs, *Phys. Rev. Lett.* **102**, 125702 (2009).  
 [11] Y. Ma, A. R. Oganov, Z. Li, Y. Xie, and J. Kotakoski, *Phys. Rev. Lett.* **102**, 065501 (2009).  
 [12] T. D. Beaudet, W. D. Mattson, and B. M. Rice, *J. Chem. Phys.* **138**, 054503 (2013).  
 [13] D. Tomasino, M. Kim, J. Smith, and C.-S. Yoo, *Phys. Rev. Lett.* **113**, 205502 (2014).  
 [14] M. I. Eremets, R. J. Hemley, H.-K. Mao, and E. Gregoryanz, *Nature (London)* **411**, 170 (2001).  
 [15] M. I. Eremets, A. G. Gavriluk, I. A. Trojan, D. A. Dzivenko, and R. Boehler, *Nat. Mater.* **3**, 558 (2004); *J. Chem. Phys.* **121**, 11296 (2004).  
 [16] B. Boates and S. A. Bonev, *Phys. Rev. Lett.* **102**, 015701 (2009).  
 [17] D. Donadio, L. Spanu, I. Duchemin, F. Gygi, and G. Galli, *Phys. Rev. B* **82**, 020102 (2010).  
 [18] A. F. Goncharov, J. C. Crowhurst, V. V. Struzhkin, and R. J. Hemley, *Phys. Rev. Lett.* **101**, 095502 (2008).  
 [19] D. Tomasino, Z. Jenei, W. Evans, and C.-S. Yoo, *J. Chem. Phys.* **140**, 244510 (2014).  
 [20] G. Weck, F. Datchi, G. Garbarino, S. Ninet, J.-A. Queyroux, T. Plisson, M. Mezouar, and P. Loubeyre, *Phys. Rev. Lett.* **119**, 235701 (2017).  
 [21] G. D. Mukherjee and R. Boehler, *Phys. Rev. Lett.* **99**, 225701 (2007).  
 [22] K. P. Driver and B. Militzer, *Phys. Rev. B* **93**, 064101 (2016).  
 [23] A. Erba, L. Maschio, C. Pisani, and S. Casassa, *Phys. Rev. B* **84**, 012101 (2011).  
 [24] J. Sun, A. Ruzsinszky, and J. P. Perdew, *Phys. Rev. Lett.* **115**, 036402 (2015).  
 [25] J. Sun, R. C. Remsing, Y. Zhang, Z. Sun, A. Ruzsinszky, H. Peng, Z. Yang, A. Paul, U. Waghmare, X. Wu, M. L. Klein, and J. P. Perdew, *Nat. Chem.* **8**, 831 (2016).  
 [26] M. Chen, H.-Y. Ko, R. C. Remsing, M. F. C. Andrade, B. Santra, Z. Sun, A. Selloni, R. Car, M. L. Klein, J. P. Perdew, and X. Wu, *Proc. Natl. Acad. Sci. USA* **114**, 10846 (2017).  
 [27] G. Kresse and J. Hafner, *Phys. Rev. B* **47**, 558(R) (1993).  
 [28] G. Kresse and J. Furthmüller, *Phys. Rev. B* **54**, 11169 (1996).  
 [29] G. Kresse and D. Joubert, *Phys. Rev. B* **59**, 1758 (1999).  
 [30] J. P. Perdew, K. Burke, and M. Ernzerhof, *Phys. Rev. Lett.* **77**, 3865 (1996).

- [31] S. Nose, *J. Chem. Phys.* **81**, 511 (1984).
- [32] L. E. Sutton, *Tables of Interatomic Distances and Configuration in Molecules and Ions* (The Chemical Society, London, 1958); B. deB. Darwent, *Bond Dissociation Energies in Simple Molecule* (National Standard Reference Data Series, National Bureau of Standards, No. 31, Washington DC, 1970); S. W. Benson, *J. Chem. Educ.* **42**, 502 (1965); K. Huber and G. Herzberg, *Molecular Spectra and Molecular Structure. IV. Constants of Diatomic Molecules* (Van Nostrand, Princeton, 1979).
- [33] A. F. Goncharov, E. Gregoryanz, H. K. Mao, Z. Liu, and R. J. Hemley, *Phys. Rev. Lett.* **85**, 1262 (2000).
- [34] S. P. Protsenko, V. G. Baidakov, and A. O. Tipseev, *Thermophys. Aeromech.* **20**, 93 (2013).
- [35] G. Zhao, Y. J. Yu, J. L. Yan, M. C. Ding, X. G. Zhao, and H. Y. Wang, *Phys. Rev. B* **93**, 140203(R) (2016).
- [36] E. S. Yakub and L. N. Yakub, *Fluid Phase Equilib.* **351**, 43 (2013).
- [37] M. Ross and F. Rogers, *Phys. Rev. B* **74**, 024103 (2006).
- [38] W. J. Nellis, N. C. Holmes, A. C. Mitchell, and M. van Thiel, *Phys. Rev. Lett.* **53**, 1661 (1984).
- [39] L. G. MacDowell, V. K. Shen, and J. R. Errington, *J. Chem. Phys.* **125**, 034705 (2006).